Supporting Information for

Construction and magnetic study of two new dysprosium complexes with chain or tetranuclear structure

Jing Yang,[a] Fang Ma,[a] Xue-Bin Deng,[a] Hao-Ling Sun,[a]* and Yi-Quan Zhang[b]*

[a] *Department of Chemistry and Beijing Key Laboratory of Energy Conversion and Storage Materials, Beijing Normal University, Beijing 100875, P. R. China. E-mail: haolingsun@bnu.edu.cn;*

[b] *Jiangsu Key Laboratory for NSLSCS, School of Physical Science and Technology, Nanjing Normal University, Nanjing 210023, P. R. China. E-mail: zhangyiquan@njnu.edu.cn.*

Experimental Section

X-ray crystallography and physical measurement

Intensity data for crystals of **1** and **2** were collected on a rigaku SuperNova, Dual, AtlasS2 diffractometer with graphite-monochromated Mo Kα radiation at 100 K. Using Olex2, the structure was solved with the olex2.solve structure solution program using Charge Flipping and refined with the olex2.refine refinement package using Gauss-Newton minimisation. All non-hydrogen atoms were refined anisotropically. Hydrogen atoms were placed at the calculation positions. The details of crystallographic data and selected bond parameters for complexes **1** and **2** are listed in Table 1 and Table S1, respectively.

Elemental analyses of carbon, hydrogen, and nitrogen were carried out with an Elementar Vario EL analyzer. FTIR spectra were recorded in the range of 4000 to 400 cm^{-1} on an AVATAR 360 Nicolet 380 FT/IR spectrometer using KBr pellets. Thermogravimetric analyses (TGA) were carried out using a Mettler-Toledo TGA/DSC1 in N_2 or air flow, from 25 ℃ to 1000 ℃, with a heating rate of 5 ℃/min.

Powder X-ray diffraction (XRD) analyses were performed on a Rigaku Dmax-2000 X-ray diffractometer with Cu Kα (λ = 1.54059 Å) radiation. Variable-temperature magnetic susceptibility measurements of **1** and **2** were performed on an SQUID-MPMS3 magnetometer.

Computational details

For CASSCF calculations, the basis sets for all atoms are atomic natural orbitals from the MOLCAS ANO-RCC library: ANO-RCC-VTZP for Dy^{3+} ion; VTZ for close O and N; VDZ for distant atoms. The calculations employed the second order Douglas-Kroll-Hess Hamiltonian, where scalar relativistic contractions were taken into account in the basis set and the spin-orbit coupling was handled separately in the restricted active space state interaction (RASSI-SO) procedure. For the fragment of Dy^{3+}, the active electrons in 7 active spaces include all *f* electrons (CAS(9 in 7) for complexes **1**–**2**) in the CASSCF calculation. To exclude all the doubts we calculated all the roots in the active space. We have mixed the maximum number of spin-free state which was possible with our hardware (all from 21 sextets, 128 from 224 quadruplets and 130 from 490 doublets for Dy^{3+} fragments).

To fit the exchange interactions in complexes **1**–**2**, we took two steps to obtain them. Firstly, we calculated one Dy^{3+} fragment using CASSCF to obtain the corresponding magnetic properties. Then, the exchange interaction between the magnetic centers is considered within the Lines model, while the account of the dipole-dipole magnetic coupling is treated exactly. The Lines model is effective and has been successfully used widely in the research field of f-element single-molecule magnets.

For complex **1**, there is only one type of *J*, and there are two types for **2**.

The exchange Hamiltonian for **1** is:

$$\hat{H}_{exch} = -J_{total}\,\hat{S}_{Dy1}\,\hat{S}_{Dy2} \qquad \text{(S1)}$$

The exchange Hamiltonian for **2** is:

$$\hat{H}_{exch} = -J_{total1}(\hat{S}_{Dy1}\,\hat{S}_{Dy2} + \hat{S}_{Dy3}\,\hat{S}_{Dy4}) - J_{total2}(\hat{S}_{Dy1}\,\hat{S}_{Dy4} + \hat{S}_{Dy2}\,\hat{S}_{Dy3}) \qquad \text{(S2)}$$

The J_{total} is the parameter of the total magnetic interaction ($J_{total} = J_{diploar} + J_{exchange}$) between magnetic center ions. The $\hat{S}_{i,y} = \pm 1/2$ are the ground pseudo-spin on the Dy^{3+} sites. The dipolar magnetic coupling can be calculated exactly, while the exchange coupling constant was fitted through comparison of the computed and measured magnetic susceptibility and molar magnetization using the POLY_ANISO program.

Table S1. Selected Bond Distances (Å) in complexes **1** and **2**

			1		
Dy1-O1	2.341(3)	Dy1-O2#1	2.366(3)	Dy1-O3#1	2.421(3)
Dy1-O3#2	2.376(3)	Dy1-O4	2.644(4)	Dy1-O5	2.520(4)
Dy1-O7	2.379(4)	Dy1-N3#1	2.535(4)	Dy1-N4#1	2.485(4)
			2		
Dy1-O1#1	2.372(3)	Dy1-O3	2.378(3)	Dy1-O5	2.315(3)
Dy1-O6	2.353(3)	Dy1-O8	2.309(4)	Dy1-O14	2.380(4)
Dy1-N7	2.519(4)	Dy1-N8	2.481(4)		
Dy2-O2	2.305(3)	Dy2-O3	2.368(3)	Dy2-O6	2.343(3)
Dy2-O7	2.324(3)	Dy2-O10	2.441(4)	Dy2-O11	2.443(4)
Dy2-N3	2.498(4)	Dy2-N4	2.442(4)		

Symmetry code for **1**:#1: -x+1, -y+1, -z, #2: x-1, y, z

Symmetry code for **2**: #1: -x+1, -y, -z+1

Table S2. Hydrogen Bonds in **1**.

D-H	d(D-H) (Å)	<DHA(°)	d(D…A) (Å)	A
C21-H21A	0.960	137.52	3.218	O6 [x+1, y, z]
C19-H19B	0.960	134.10	3.320	O8
C9-H9	0.930	161.51	3.370	O5 [x+1, y, z]

Table S3. Hydrogen Bonds in **2**.

D-H	d(D-H) (Å)	<DHA(°)	d(D…A) (Å)	A
C9-H9	0.930	155.30	3.364	O11 [-x+1, -y, 1-z]
C35-H35A	0.930	148.98	3.218	O4 [-x+1, -y, 1-z]
C2-H2	0.930	159.60	3.357	N6

Table S4. Relaxation fitting parameters from Least-Squares Fitting of $\chi(f)$ data under zero dc field of **1**.

T (K)	χ_s	χ_t	α	τ
2	13.8	3.13	0.107	4.65E-4
2.2	12.3	2.97	0.090	4.42E-4
2.4	11.1	2.77	0.083	4.11E-4
2.6	10.1	2.60	0.074	3.76E-4
2.8	9.28	2.47	0.065	3.38E-4
3	8.57	2.32	0.060	2.95E-4
3.2	7.97	2.13	0.061	2.50E-4
3.4	7.45	1.97	0.060	2.08E-4
3.6	6.99	1.76	0.068	1.67E-4
3.8	6.57	1.94	0.049	1.50E-4
4	6.2	1.89	0.060	1.24E-4

Table S5. Relaxation fitting parameters for Cole-Cole plots of using the sum of two modified Debye functions under 2 kOe dc field of **1**.

T (K)	χ_s	χ_t	β	τ_1	α_1	τ_2	α_2
2	0.67	11.13	0.53	0.28	0.35	0.002	0.46
2.2	0.72	10.46	0.46	0.25	0.32	1.70E-3	0.42
2.4	0.78	9.16	0.35	0.16	0.24	1.40E-3	0.39
2.6	0.85	8.50	0.29	0.14	0.19	1.00E-3	0.34
2.8	0.96	8.28	0.30	0.16	0.28	8.50E-4	0.28
3.0	1.01	7.79	0.27	0.15	0.35	6.40E-4	0.23

T (K)	χ_s	χ_t	α	τ
3.2	0.88	6.12	0.25	5.14E-4
3.4	0.81	5.95	0.24	3.68E-4
3.6	0.65	5.77	0.24	2.56E-4
3.8	0.41	5.59	0.25	1.73E-4
4.0	0.42	5.37	0.24	1.28E-4

Table S6. Calculated energy levels (cm^{-1}), $\boldsymbol{g}(g_x, g_y, g_z)$ tensors and m_J values of the lowest Kramers doublets (KDs) of the Dy^{3+} fragments of complexes **1**–**2**.

KDs	**1**			**2(Dy1)**			**2(Dy2)**		
	E	*g*	m_J	*E*	*g*	m_J	*E*	*g*	m_J
1	0.0	0.026 0.113 17.547	±15/2	0.0	0.081 0.995 18.073	±15/2	0.0	0.085 0.152 19.136	±15/2
2	46.0	0.810 0.956 14.501	±13/2	40.0	0.007 1.270 17.464	±1/2	59.0	0.595 5.120 14.665	±1/2
3	79.5	0.223 1.081 16.546	±7/2	129.8	3.783 5.969 9.003	±5/2	92.2	1.955 3.012 11.171	±5/2
4	150.0	3.822 5.010 11.792	±5/2	149.6	1.855 2.472 12.960	±3/2	122.4	0.352 1.187 14.814	±13/2
5	186.4	1.124 2.821 14.020	±11/2	228.5	2.610 3.194 9.609	±9/2	198.8	1.269 4.191 13.265	±11/2
6	210.1	0.089 2.335 14.280	±9/2	262.5	1.530 4.411 12.148	±7/2	232.5	10.047 6.943 2.803	±3/2
7	267.9	1.106 1.507 14.015	±1/2	349.2	0.230 0.788 16.965	±11/2	329.4	0.585 1.354 13.290	±7/2
8	389.1	0.062 0.146 18.795	±3/2	391.8	0.244 0.715 18.354	±13/2	407.6	0.352 1.446 17.080	±9/2

Table S7. Calculated exchange energies (cm^{-1}), the corresponding tunneling gaps (cm^{-1}) and the main values of the g_z for the lowest two exchange doublets of **1** and eight of **2**.

KDs	**1**			**2**		
	E	Δ_{tun}	g_z	E	Δ_{tun}	g_z
1	0.000	1.279×10^{-4}	35.123	0.000	1.857×10^{-5}	37.332
2	0.657	1.450×10^{-4}	0.000	1.169	1.223×10^{-5}	0.000
3				1.708	2.937×10^{-4}	0.000
4				1.710	2.766×10^{-5}	0.000
5				1.722	7.988×10^{-5}	0.000
6				1.724	1.346×10^{-4}	0.000
7				2.277	1.870×10^{-5}	0.000
8				3.417	2.463×10^{-5}	63.735

Table S8. Parameters of the magnetic interactions between Dy^{3+} ions in **1**–**2** (cm^{-1}). The intermolecular interactions zJ' of **1**–**2** were fit to −0.01 and 0.01 cm^{-1}, respectively.

		1	**2**	
			Dy1-Dy2/ Dy3-Dy4	Dy1-Dy4/ Dy2-Dy3
J	$J_{dipolar}$	3.58	2.25	−0.13
	J_{exch}	−3.00	−5.32	−1.21
	J	0.58	−3.07	−1.34

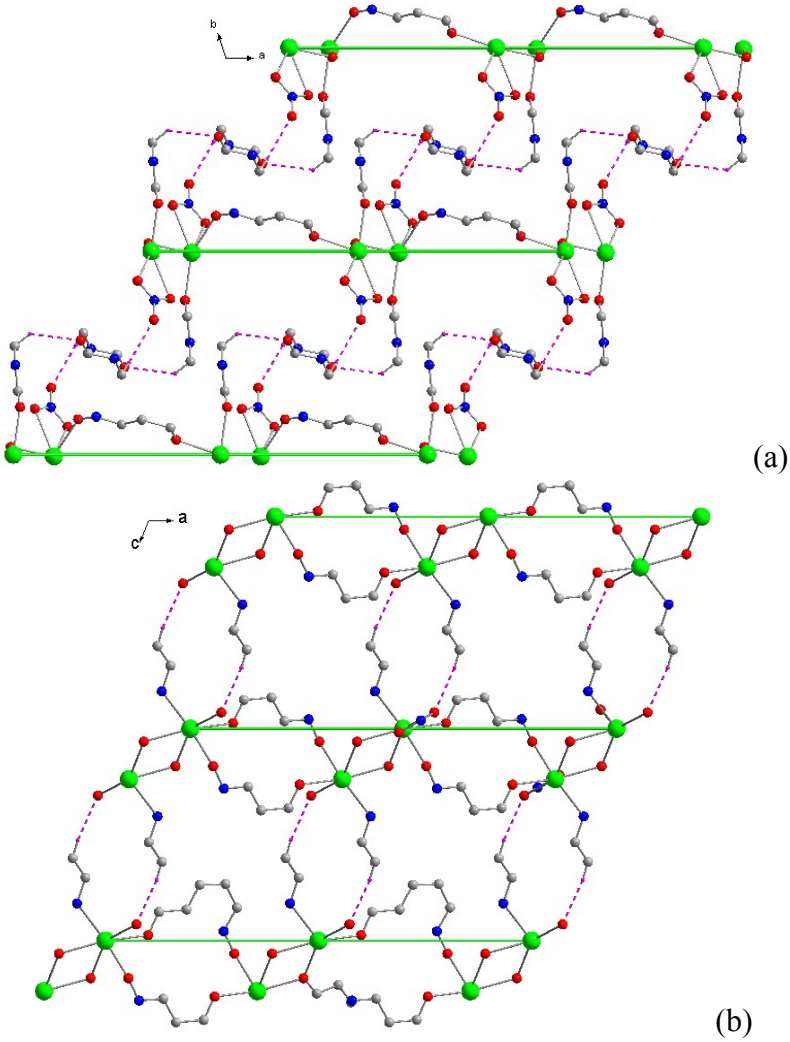

Fig S1. The 2D structure constructed by hydrogen bonds in the *ab* plane (a) and the hydrogen bonds between the layers along the *c*-axis (b) of complex **1** (gray, C; red, O; blue, N; turquoise, H; and green, Dy).

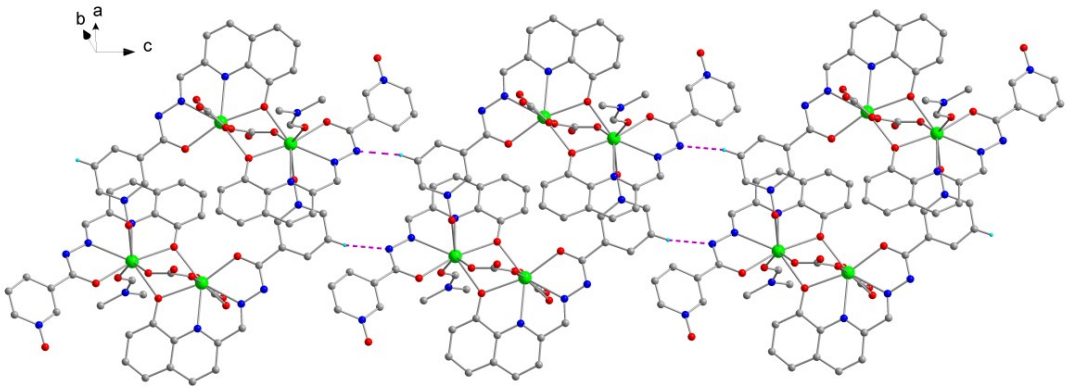

Fig S2. 1D chain of complex **2** constructed by hydrogen bonds. (gray, C; red, O; blue, N; turquoise, H; and green, Dy).

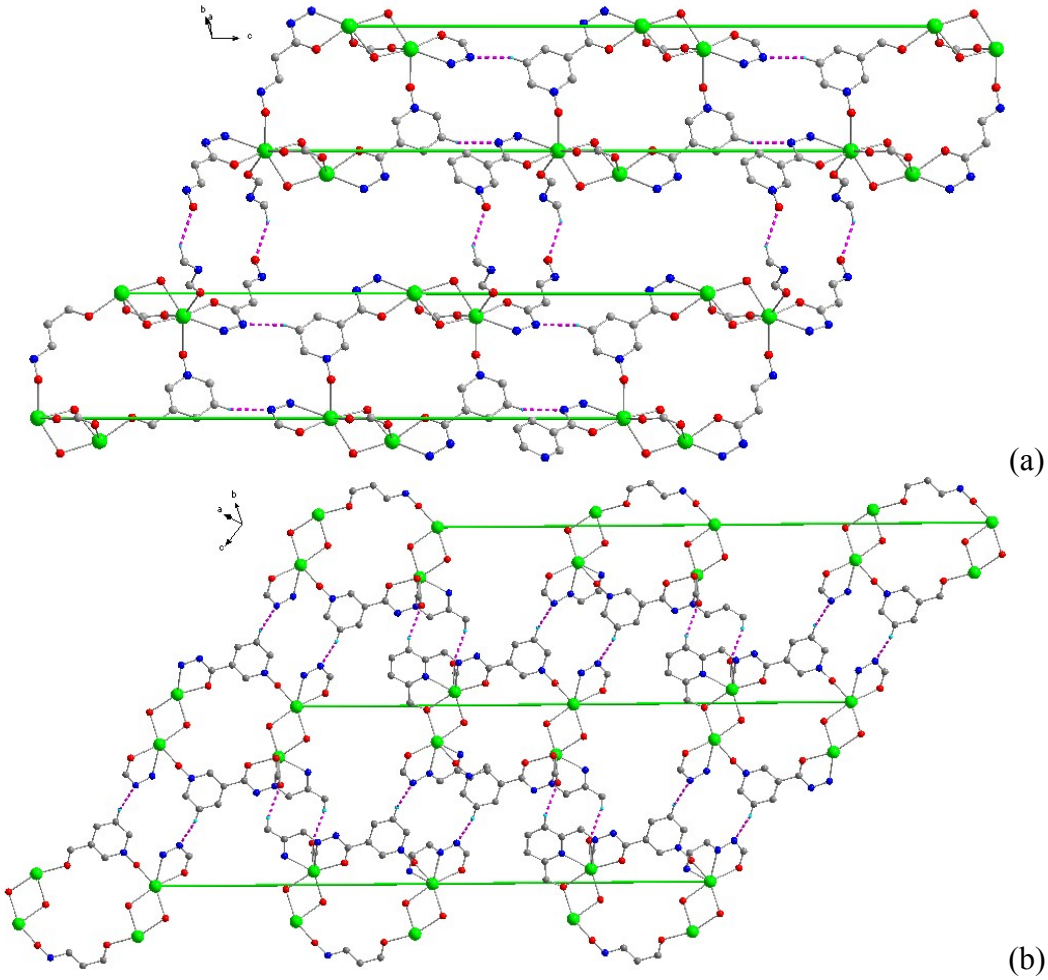

Fig S3. The 2D structure constructed by hydrogen bonds in *ac* plane (a) and the hydrogen bonds between the layers along the *c*-axis (b) of complex **2** (gray, C; red, O; blue, N; turquoise, H; and green, Dy)

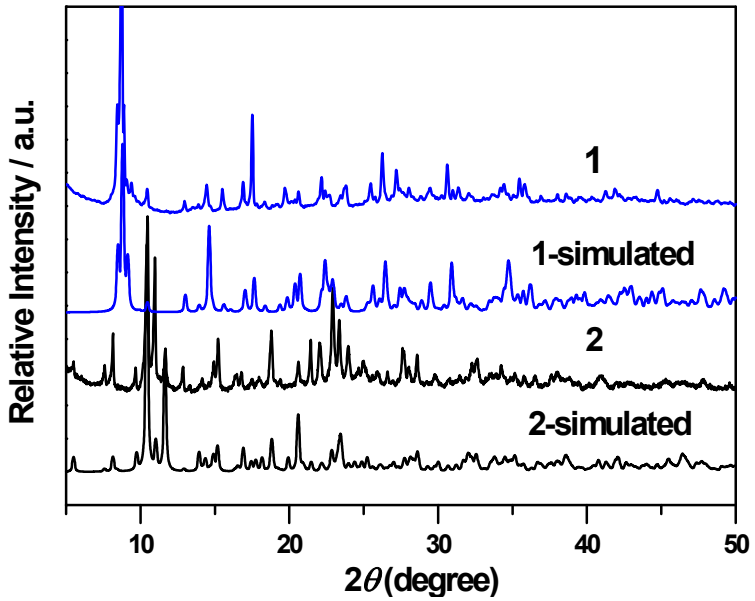

Fig. S4 Powder X-ray diffraction profiles of **1**-**2** together with simulations from the single crystal data

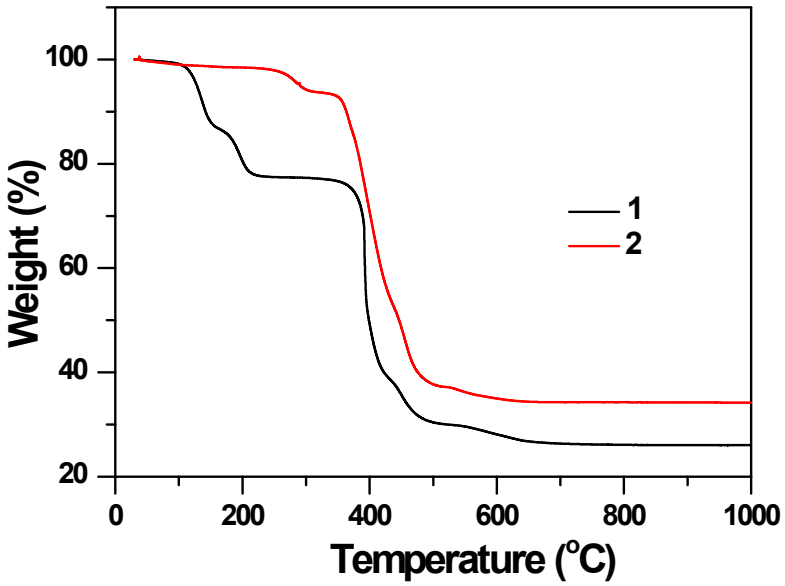

Fig. S5. TGA curves of complex **1** and **2**.

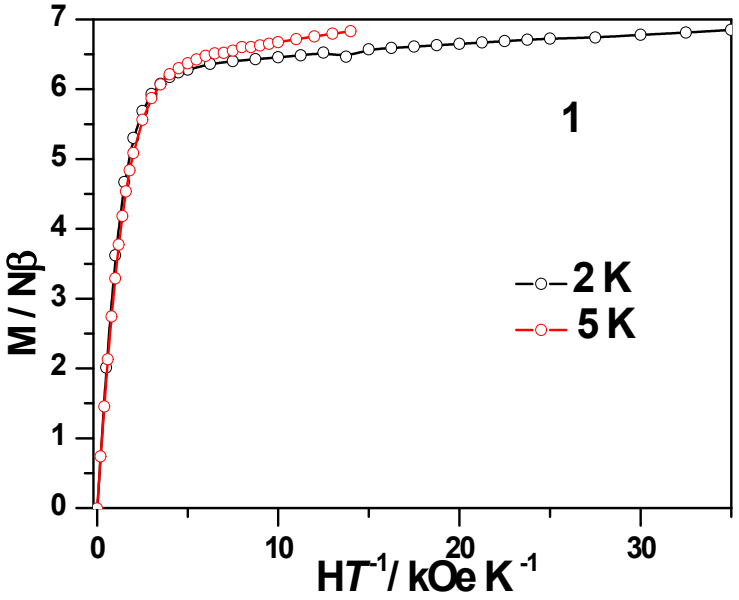

(a)

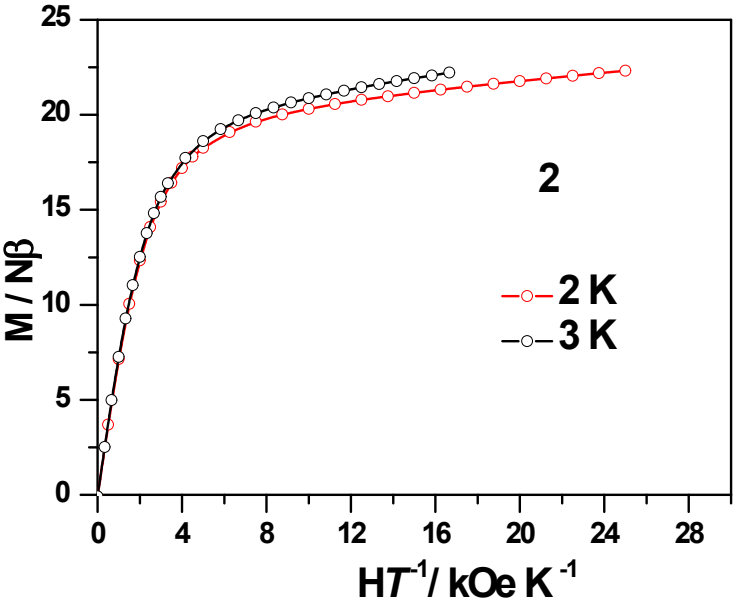

(b)

Fig. S6 Plots of *M*-*H* for **1** (a) and **2** (b), respectively.

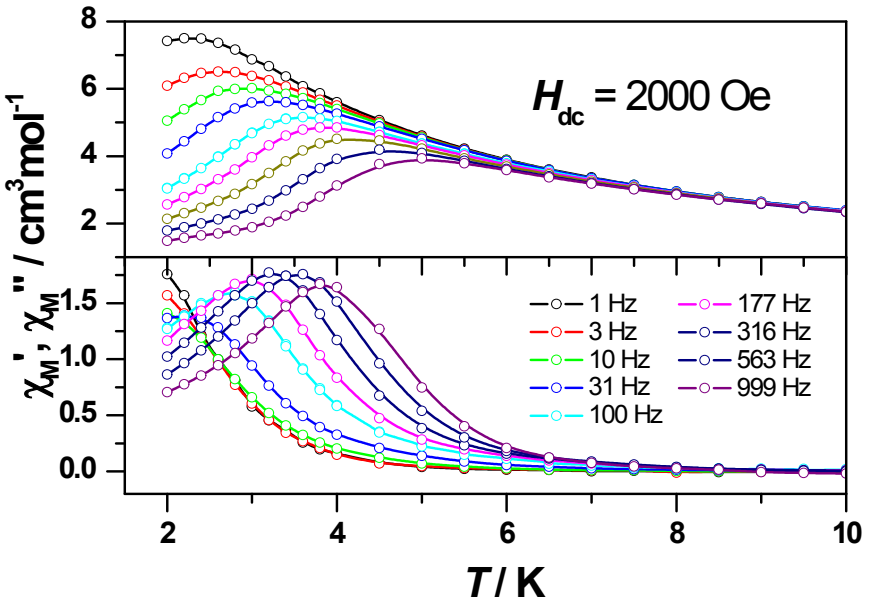

Fig. S7 The temperature dependence of ac susceptibility under 2 kOe field for **1.**

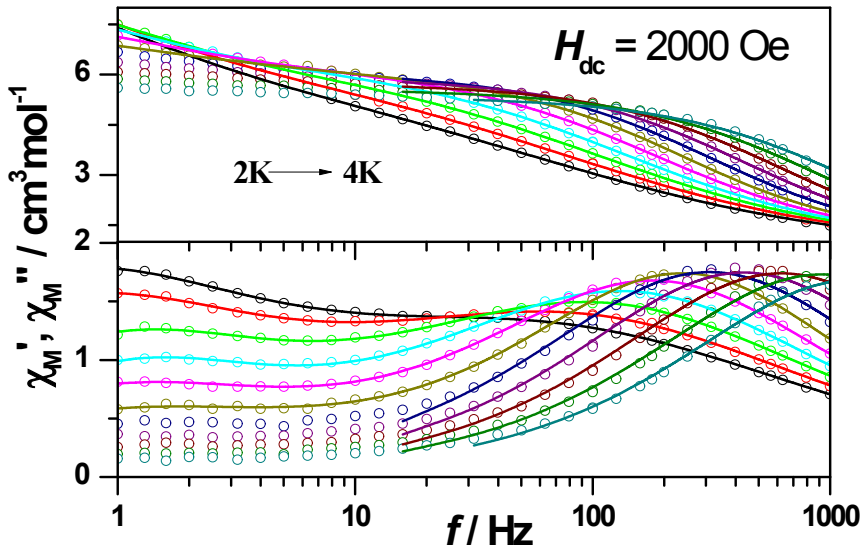

Fig. S8 $\chi''(f)$ curves measured under 2 kOe field for **1** at selected temperatures. Solid lines were fitted using a generalized Debye relaxation model.

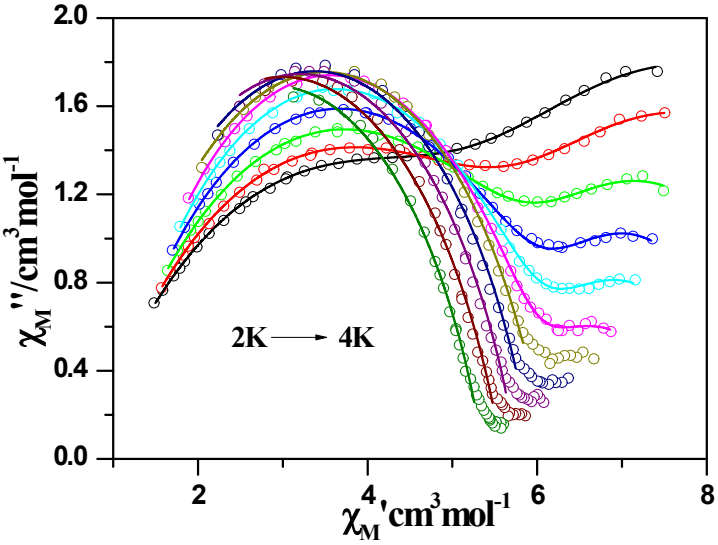

Fig. S9 Cole-Cole plots measured at 2.0-4.0 K under 2 kOe dc fields for **1**. Solid lines show fitting curves.

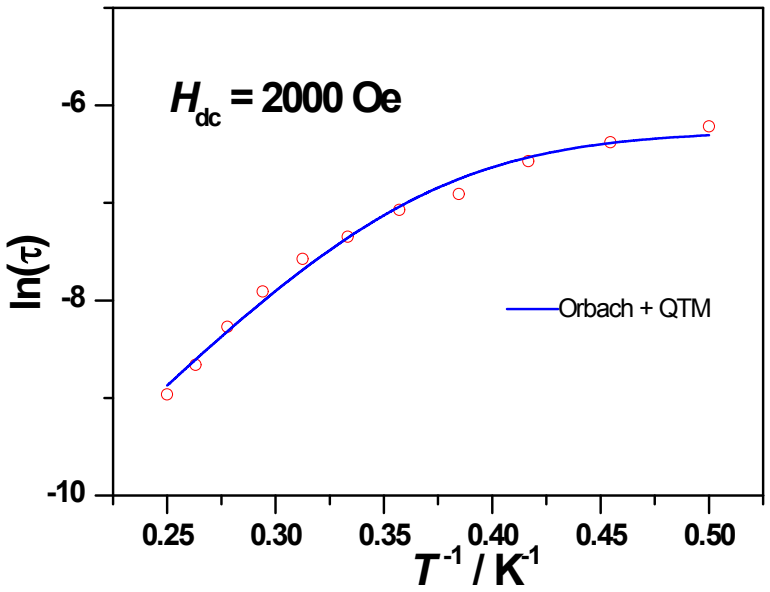

Fig. S10 Plots of ln τ vs. T^{-1} for **1** under 2 kOe dc field.

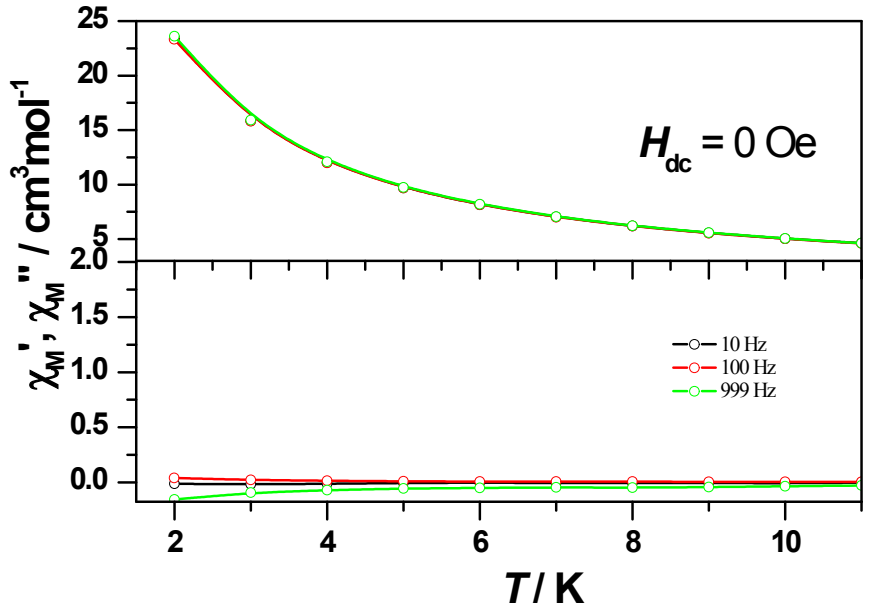

Fig. S11 The temperature dependence of ac susceptibility under zero field for **2.**

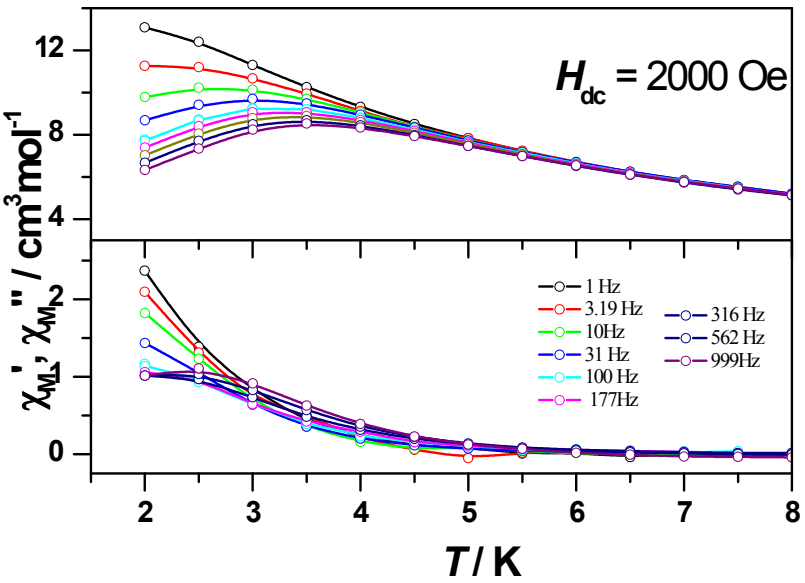

Fig. S12 The temperature dependence of ac susceptibility under 2 kOe field for **2.**

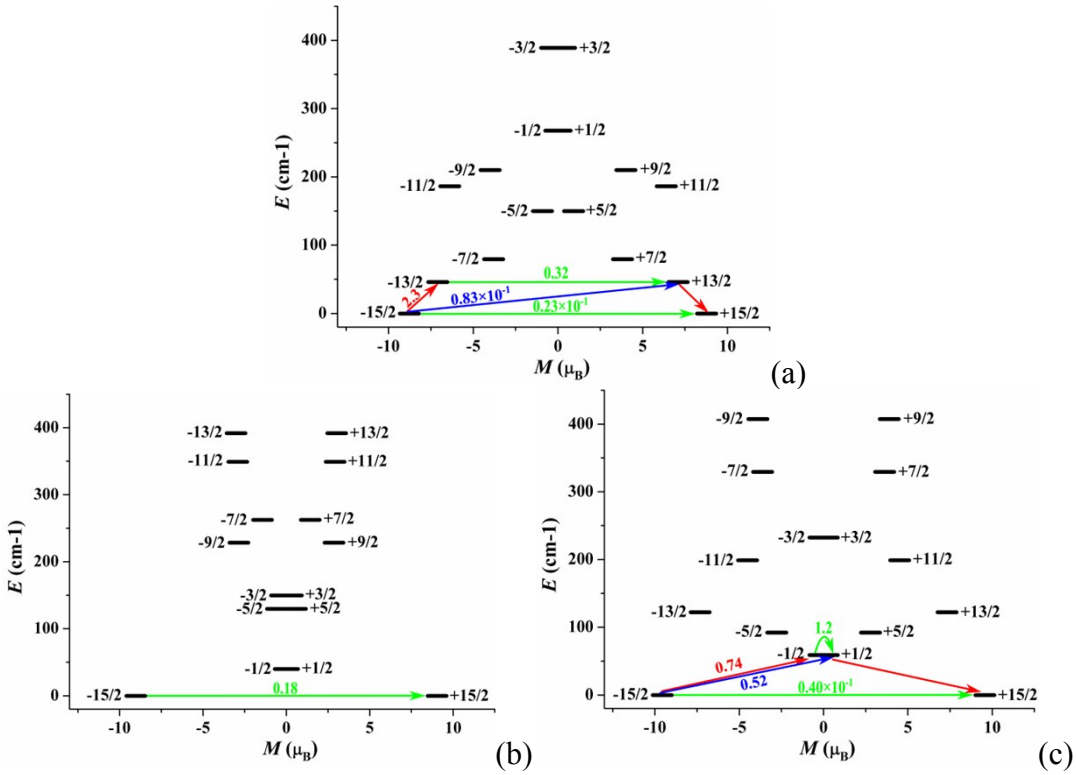

Fig. S13. The magnetization blocking barriers for individual Dy^{3+} fragment of complexes **1**–**2** (one type of Dy^{3+} fragment for **1**(a), and two types of Dy^{3+} fragments for **2**(b for $Dy1^{3+}$, c for $Dy2^{3+}$)). The thick black lines represent the Kramers doublets as a function of their magnetic moment along the magnetic axis. The green lines correspond to diagonal quantum tunneling of magnetization (QTM); the blue line represent off-diagonal relaxation process. The numbers at each arrow stand for the mean absolute value of the corresponding matrix element of transition magnetic moment.